Fission Fragment Tracking and Identification in the Neutron-Induced Fission Fragment Tracking Experiment's Time Projection Chamber

A Senior Project

presented to

the Faculty of the Physics Department

California Polytechnic State University, San Luis Obispo

In Partial Fulfillment

of the Requirements for the Degree

Bachelor of Science

by

Eric Song

March, 2015

Abstract: The Neutron-Induced Fission Fragment Tracking Experiment (NIFFTE) built a novel Time Projection Chamber (TPC), the FissionTPC, for measuring neutron-induced fission cross-sections to unprecedented precision. We investigated data from a 2014 run (400010151) at the Los Alamos Neutron Science Center (LANSCE) with a double-sided U235/Pu239 target. Our particle identification studies will aid in the development of improved tracking algorithms.

1. Introduction

Nuclear fission is the process of splitting an atom into two, possibly three fragments, often using an incident neutron.[1] The cross section is the probability of inducing fission, related to the atomic nucleus and the incident energy of the neutron.[2] Atoms consist of electrons (negative charge) and the nucleus, which consists of protons (positive charge) and neutrons (no charge). An element's identity is determined by the number of protons in each atom's nucleus, called the "atomic number." Different isotopes of the same element have the same atomic number but a different number of neutrons. The Strong Nuclear force holds the nucleus together against the Electromagnetic force which otherwise would make the protons repel each other while the weak nuclear force governs the process of radioactive decay.[3]

Fission cross sections need to be measured to better than 1% precision to increase efficiency and minimize waste in nuclear reactors.[4] Figure 1 shows the world's data from neutron induced fission of Pu-239 relative to U-235 as a function of neutron energy. The green line represents a 1% uncertainty around the calculate average. As is evident, there is considerable discrepancy between data points from different experiments. The Neutron Induced Fission Fragment Tracking Experiment (NIFFTE) aims to address these discrepancies by applying a novel technology to the investigation of fission reactions.[5]

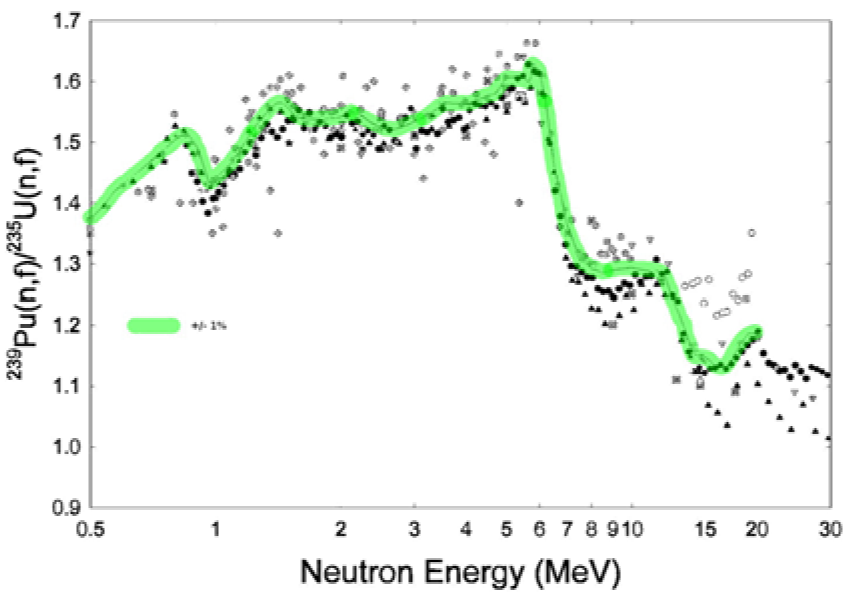

Figure 1: Data Points and Average for ^{239}Pu/^{235}U Neutron Induced Fission Cross Section Ratio[4]

Radioactive nuclei have a disproportionate neutron to proton (n:p) ratio or contain excess nucleons (protons and neutrons). In massive nuclei with a large number of nucleons, the difference between binding energy from the strong nuclear force and the repulsion from the electromagnetic force becomes smaller with larger nuclei.[6] At large enough nuclei, the binding energy is less than the repulsive energy, resulting in an unstable nucleus.[6] Stable nuclei generally have a n:p ratio of around 1:1. Stable elements with atomic numbers 20 to 60 have a n:p ratio of ~1.2, elements with 60 to 83 protons have a n:p ratio of ~1.5, and those with atomic numbers greater than 83 are generally unstable. This n:p trend, known as the "belt of stability", is shown in Figure 2 from UC Davis.[7]

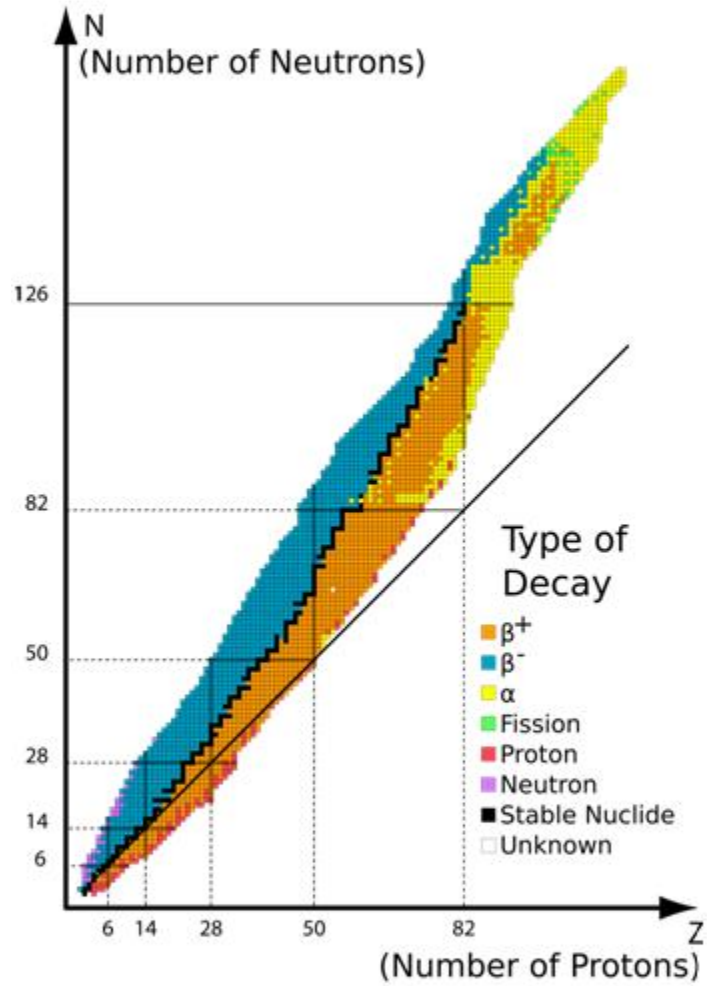

Figure 2: Belt of Stability for Atomic Nuclei with Decay Types[7]

Unstable nuclei undergo decay to achieve a more stable state, generally by adjusting the n:p ratio or by becoming less massive.[8]

Alpha decay is when a nucleus emits an alpha particle; a Helium nucleus with +2 electric charge. An example alpha decay is:

$$^{222}_{88}Ra \rightarrow {}^{4}_{2}He + {}^{218}_{86}Rn$$

Alpha decay occurs with massive nuclei (>83 protons).

Beta decay occurs when a nucleus emits an electron and electron antineutrino (beta-) or a positron and electron neutrino (beta+). Example beta minus and beta plus decays are shown below:

$$^{137}_{55}Cs \rightarrow {}^{137}_{56}Ba + e^{-} + \overline{\nu_e}\ (beta\ minus)$$
$$^{22}_{11}Na \rightarrow {}^{22}_{10}Ne + e^{+} + \nu_e\ (beta\ plus)$$

Beta minus decay occurs when the nucleus' n:p ratio is above the belt of stability and beta plus decays occurs when the n:p ratio is below the belt of stability. To adjust the n:p ratio, a neutron turns into a proton and neutron in beta minus decay, while a proton decays into a neutron and positron in beta plus.[8]

Another method of adjusting the n:p ratio is by electron capture, example below:

$$^{81}_{36}Kr + e^- \rightarrow {}^{81}_{35}Br + \nu_e$$

An electron merges with a proton in the nucleus to form a neutron and the resulting nucleus emits an electron neutrino. In all cases, an electron neutrino or antineutrino is emitted to conserve lepton number.[9]

One method to visualize fission is the "liquid drop model." The nucleus is analogous to a water drop; too massive a water drop means the surface tension can't contain the mass of the drop so it splits. The same idea applies with fission; too massive a nucleus splits because the binding energy can't hold the nucleons together. Incident neutrons in fission reactions add mass to already unstable nuclei, causing the nucleus to split and release energy in the process. A common fissionable nucleus is Uranium 235 (U-235) since the incident neutron energy is greater than the nucleus' critical energy.[2] Figure 3 shows an example fission reaction where a neutron excites a nucleus which splits into a heavy and light mass fragment which may further de-excite and/or decay into a stable final state.

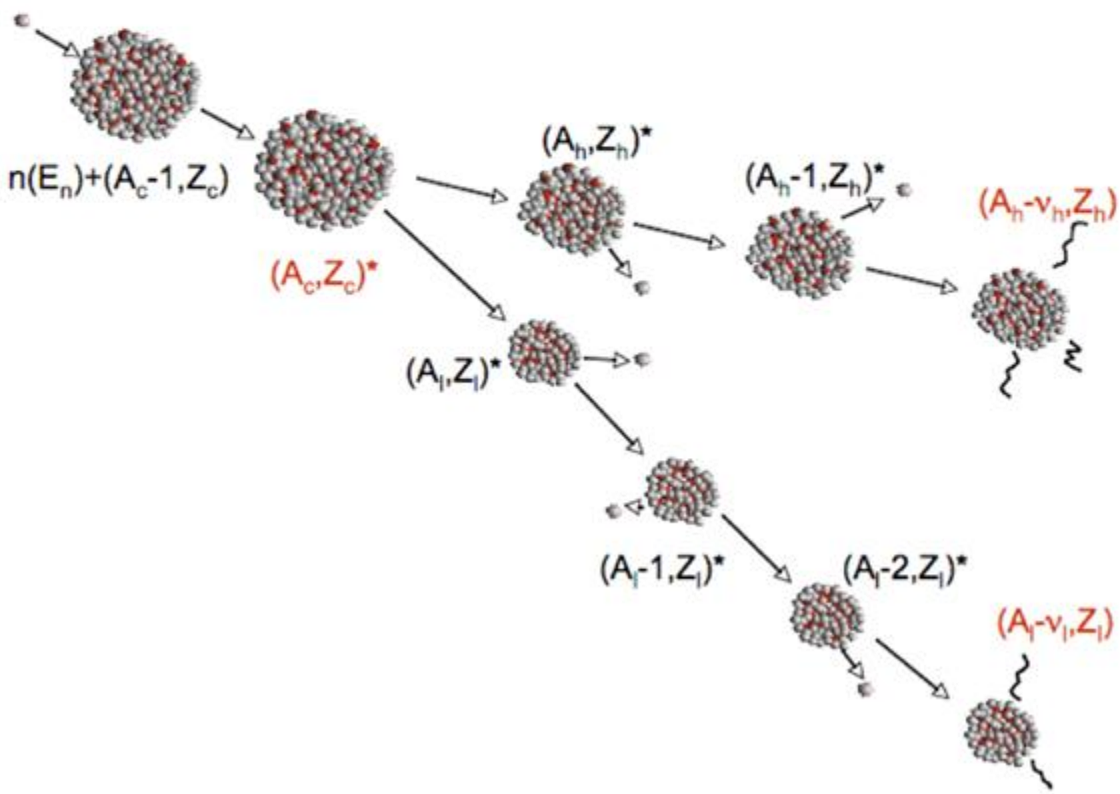

Figure 3: Neutron Induced Fission and Radioactive Decay Steps[10]

As decay products travel, they deposit energy into their surroundings. More massive decay products like fission fragments deposit more energy per length and smaller products such as alphas deposit less. One can plot the energy deposited vs. penetration distance in a Bragg

Peak/Curve.[10] A typical Bragg curve for alpha particles in air is shown in Figure 4.

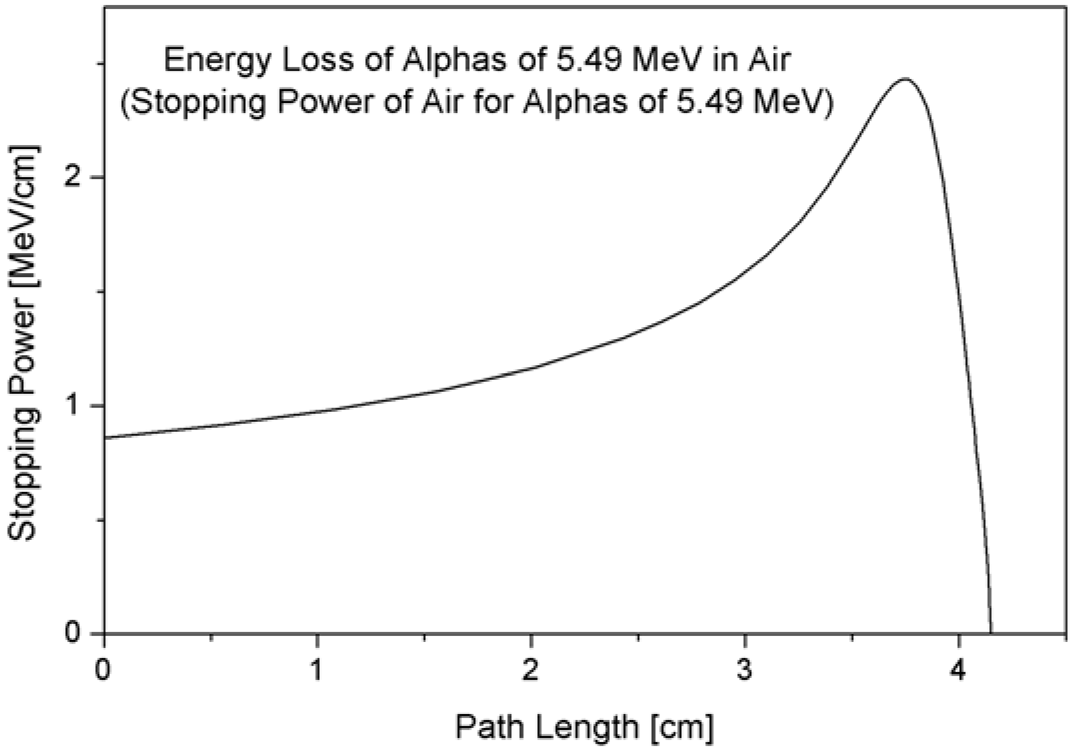

Figure 4: Energy Loss for Alpha Particles in Air[10]

The ionization energy loss is peaked near the end of the particle's path because the cross-section increases as the energy of the alpha decreases. For fission fragments, the stopping power is much higher and the fragments travel less far within a given medium. Fragments from U235 and Pu239 fission generally have similar masses. The nucleus breaks into two fragments, one with a higher mass and one with a lower mass, as seen previously in Figure 3. For an ensemble of fission events, one can plot the frequency of occurrence vs. atomic mass, as in Figure 5 from Ref. 2.

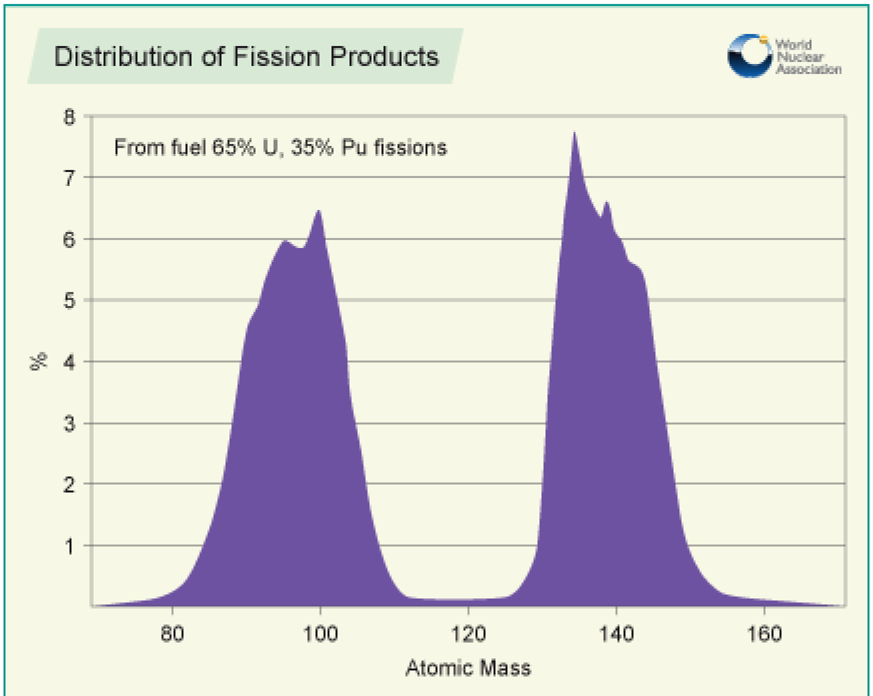

Figure 5: Probability vs. Atomic Mass Plots for Fission Fragments[2]

In a cross-section measurement experiment, one compares the rate of neutron-induced fission events to the number of incident neutrons to accurately determine the probability of the reaction. In order to count the fission reactions, one must be able to efficiently detect and distinguish different types of particles. The NIFFTE TPC allows one to do this by creating a 3-dimensional image of the reactions where particle trajectories and identities can be determined.

2. Experimental Method

The Neutron Induced Fission Fragment Tracking Experiment (NIFFTE) at Los Alamos National Lab (LANL) will be using a Time Projection Chamber (TPC) for its measurements.[12] A standard TPC is a gas filled volume with a cathode in the center and anodes on each end. Charged particles ionize the gas atoms. The ionization clouds can then be measured by drifting the ionization in a uniform electric field to a charge-sensitive detection plane. Traditional TPCs also employ a magnetic field to bend the particles. One can calculate the momentum of the particle from the curvature. In NIFFTE's TPC there is no magnetic field so momentum is not measured.[5]

The NIFFTE TPC, also called the FissionTPC, is made of two small gas volumes separated by a target plane with a holder for placing a thin layer of radioactive targets in the middle. A copper field cage surrounds the space for the reaction to take place, and a mixture of 95% Argon and 5% Isobutane gas fills the inside volume. The target plane in the center is the cathode plane and the two ends of the detector are anode planes with a -300V MICROMEGAS amplification region above a hexagonally-segmented pad plane. The pads are approximately 2mm x 2mm and are read out by 192 "EtherDaq" cards, each handling signals from 32 hexagonal pads.[5] A cutaway view of the FissionTPC chamber is shown in Figure 6:

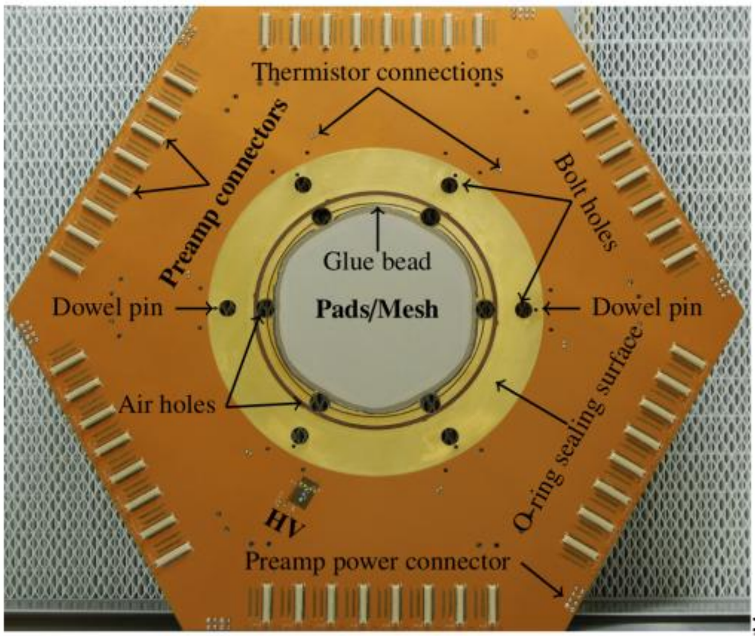

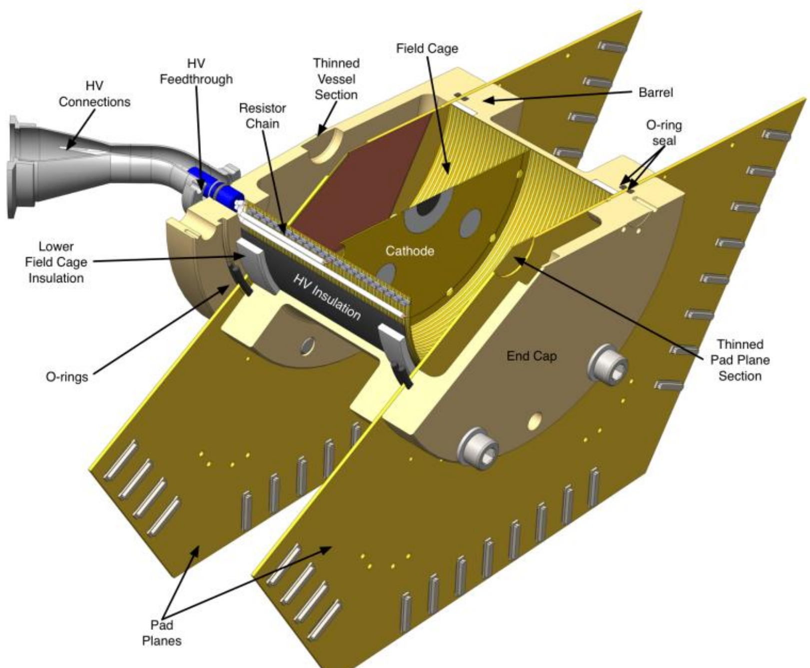

Figure 6: Cutaway View of the FissionTPC Design[5]

The experiment is operated in the 90-left flight path of the Weapons Neutron Research section of the Los Alamos Neutron Science Center with a "white" source neutron beam. The neutrons are created from the collision of a high energy proton beam with a tungsten target that produces neutrons of a spectrum of energies up to the maximum allowed by the beam. In order to determine the energy of the neutron that produced a fission reaction, one measures the time-of-flight for the neutron from the source to the FissionTPC target plane.[5]

After neutrons from a neutron beam cause a fission reaction, the resulting particles are measured by looking at the energy deposited and the distance traveled. Smaller particles like alphas and protons will have longer tracks but will deposit less energy per length. Larger particles like fission fragments will have shorter tracks but will deposit more energy per length. Figure 7 shows an example of an alpha-accompanied fission event in the NIFFTE TPC. Note, volumes 0 and 1 denote each half of the chamber. Several advanced pattern recognition algorithms are available to find the tracks left by the ionizing particles. Subsequent track fitting algorithms are then used to determine the track parameters, such as the start/end points, specific ionization along the track, its direction, and track length.[5]

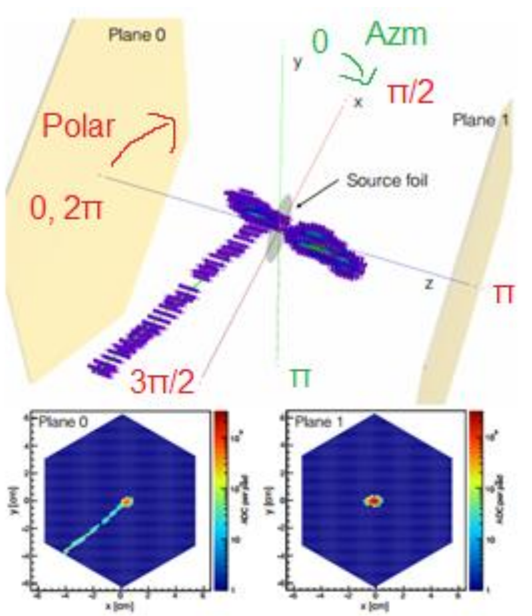

Figure 7: An alpha-accompanied fission event detected as a 3-dimensional image in the NIFFTE TPC. Note; volumes 0 and 1 denote each half of the chamber. The Azimuthal Angle, Polar Angle, and XY Plane are also indicated.

The left and right panels of Figure 8 show Bragg curves for fission fragments and alphas detected in the NIFFTE TPC. The difference in magnitude of the ionization, track lengths, and locations of the Bragg peaks can all be used to distinguish fragments from alphas. The research included in this report used the track length vs. total energy (area under the curves in Figure 8) in terms of ADC counts measured by the FissionTPC to investigate the tracking performance for different types of particles. Details of the data and analysis will be presented in Sections 3 and 4.

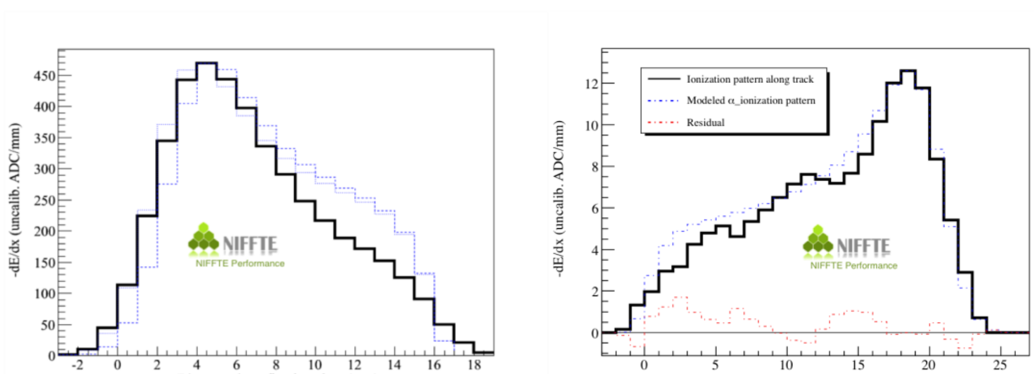

Figure 8: Specific ionization along the track for a fission fragment (left) and an alpha (right) detected in the NIFFTE TPC compared to numerical simulations (dashed curves).

3. Data/Results

In this section, we show data from Run 40010151 (10151 for short), taken on Nov 12, 2014 12:49 to 1:00 pm PST using 5% Argon and 95% Isobutane, with a double-sided target in neutron beam at LANSCE. A thin film of U-235 was deposited on the target inside Volume 0 while a thin film of Pu-239 was deposited on the target inside Volume 1. Figure 9 shows Length vs. ADC for all tracks detected in the two different volumes, with lines dividing the regions into high mass fission fragments, low mass fission fragments, and smaller particles (alphas, protons, recoil ions, etc.). The orange line separates the low and high mass fission fragments and the vertical red line separates the fragments from everything else. The dark red in the color plots represents where the largest number of tracks occurred. The concentrated spots near track lengths of 5 cm and ADC 1000 are alpha particles produced with a characteristic energy. The distance traveled in the gas depends on the gas type, temperature, and pressure.[5]

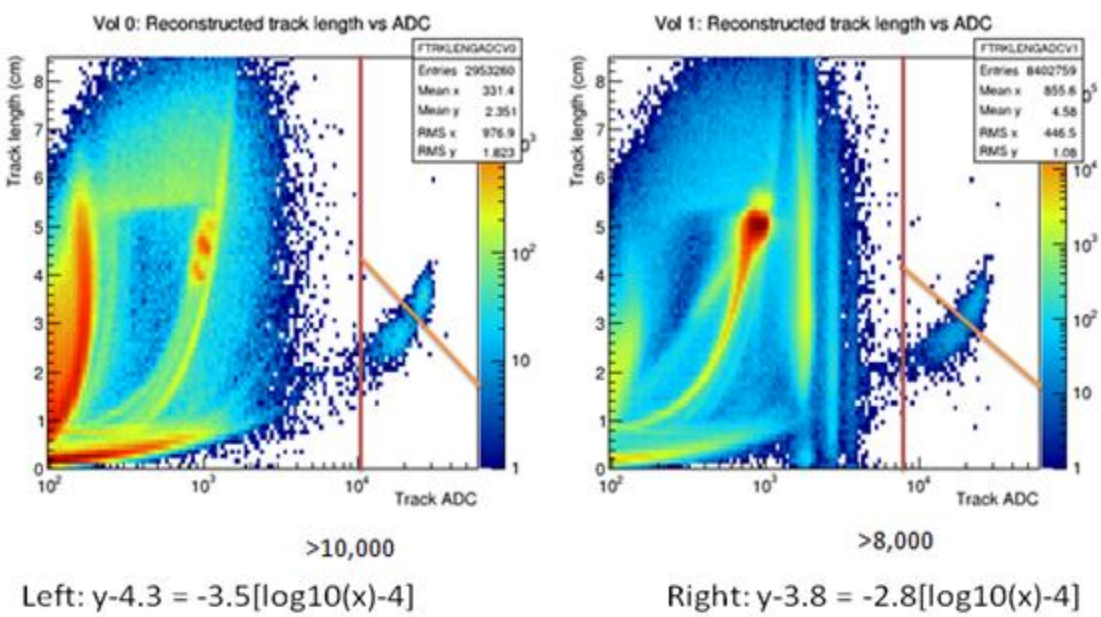

Figure 9: Run 10151 with Fission Fragments and Cut Equations

ADC is a measure of the energy deposited per length of track and the ADC axis is on a $\log_{10}$ scale. Higher mass fragments deposit more energy per length so they statistically lose all their energy faster. This can be seen in the plot, where the high mass fission fragments are on the lower left, meaning higher energy deposits but at shorter track length, and the smaller fragments are along the left side, meaning they deposit less energy along a longer distance. The high mass fission fragments are more towards the upper right than the low mass fission fragments.

Setting Track ADC to a value sets the vertical line dividing the fragments from lighter particles. A line in point-slope form

$$y - y_0 = m(\log_{10} x - \log_{10} x_0) \quad (1)$$

defines the diagonal line separating the high mass fission fragment from the low mass fission fragment. In the equation, y is the Track Length, x is the Track ADC, and (x_0, y_0) is an arbitrary point on the graph to calculate m, which is the slope of the graph (always negative value). We chose $x_0 = 10000$ and x = 1000 for all the runs, so $\log_{10} x - \log_{10} x_0 = -1$. Thus the slope equation $m = \frac{y-y_0}{\log_{10} x - \log_{10} x_0}$ reduces to $y_0 - y$, where y is the Track Length at x=1000 and y_0 is the Track length at x=10000.

Figure 10 shows further cuts for the lighter particles in volumes 0 and 1 for Run 10151.

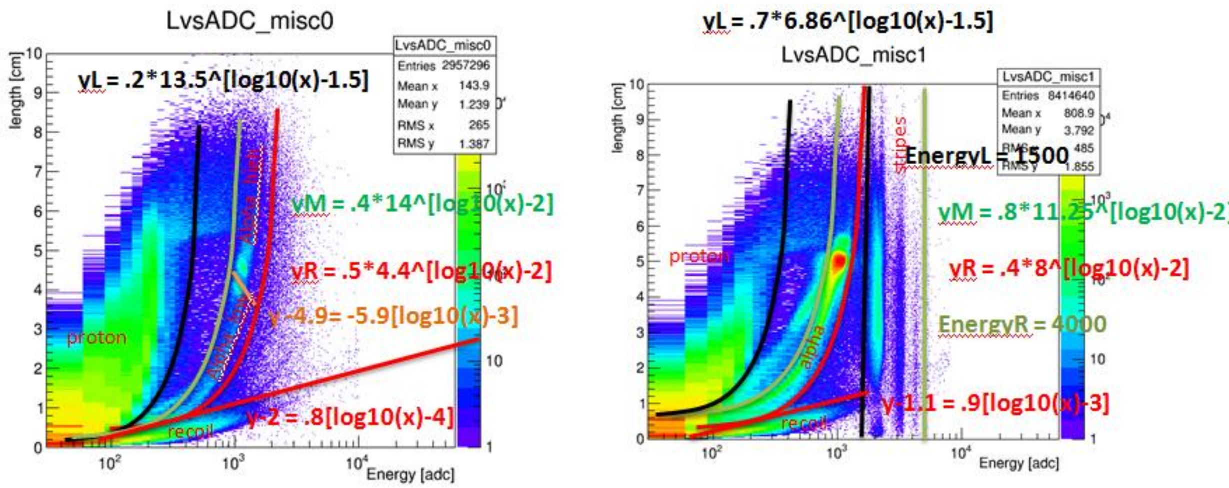

Figure 10: Cuts and Equations for Lighter Particles

The diagonal lines in Figure 10 are derived the same way as the line in Figure 9. The exponential curve equations in Figure 10 are in the form

$$y = A * B^{\log_{10} x - \log_{10} x_0} \quad (2)$$

where y is Track Length, x is Track ADC, and A is the Track Length at an arbitrary Track ADC x_0. To calculate B, first choose an x_0 and find the associated Track Length, A, by visual examination of a curve. Then pick another arbitrary x and find the Track Length at that x, call this variable z. We then obtain

$$B = \left(\frac{z}{A}\right)^{\frac{1}{\log_{10} x - \log_{10} x_0}} \quad (3)$$

For example, to obtain yR in volume 1 from Figure 10, we chose $x_0 = 100\ and\ x = 1000$, thus $A = .4\ and\ z = 3.2$. Plugging in the values, we calculate

$$B = \left(\frac{z}{A}\right)^{\frac{1}{\log_{10} x - \log_{10} x_0}} = \left(\frac{3.2}{.4}\right)^{\frac{1}{\log_{10} 10^3 - \log_{10} 10^2}} = .8^1 = .8 \quad (4)$$

$$yR = .4 * .8^{\log_{10} x - 2} \quad (5)$$

To simplify the calculations, we chose x and x_0 values such that $\log_{10} x - \log_{10} x_0 = \pm 1$ so

$$B = \begin{cases} \frac{z}{A}, & x > x_0\ (\log_{10} x - \log_{10} x_0 = 1) \\ \frac{A}{z}, & x < x_0\ (\log_{10} x - \log_{10} x_0 = -1) \end{cases} \quad (6)$$

For both the lines and the exponential curves, some trial and error may be necessary if the cuts don't give the desired results since there will be some uncertainty in visual examination measurements. In the next section we identify the sources of the different regions delineated here and use the cuts to investigate the track parameters for different types of particles.

4. Analysis

Using the cut regions outlined in Section 3, we examine the angular distributions for the different particle types by plotting the cosine of the polar angle (measured from the beam line, the Azimuthal angle and the start and end points in the X-Y plane, as depicted in Figure 7. The Polar Angle goes from 0 to 2π along the XZ plane, the Azimuthal Angle goes from 0 to π along the YZ plane. StartXY and EndXY are the count distributions along the XY plane at the start and end of the reaction path along the Z axis respectively. Figure 9 has the Polar Angle labeled in red, Azimuthal (Azm) labeled in green, and both with arrows pointing in the direction of increasing angle.

Figures 11 and 12 show the angular distributions for the different cut regions in volume 0 and 1, respectively. The upper left panel is the uncut length vs. ADC while the upper right shows the different color-coded cut regions. In both volumes; red is the low mass fission fragment, light green is the high mass fission fragment, yellow is the proton, dark green is the recoil, and blue isn't identified yet. In Volume 0; purple is the low energy alpha and teal is the high energy alpha. In Volume 1; purple is the alpha and teal is the stripe. Higher track ADC, or to the right on the horizontal axis, means more energy deposited per unit volume along the track. Increasing track length, or distance traveled, means moving up on the vertical axis. Note, L vs. ADC is track length vs. ADC, CosPolar is the distribution with respect to Cosine of the Polar Angle, Azm is distribution with respect to the Azimuthal angle.

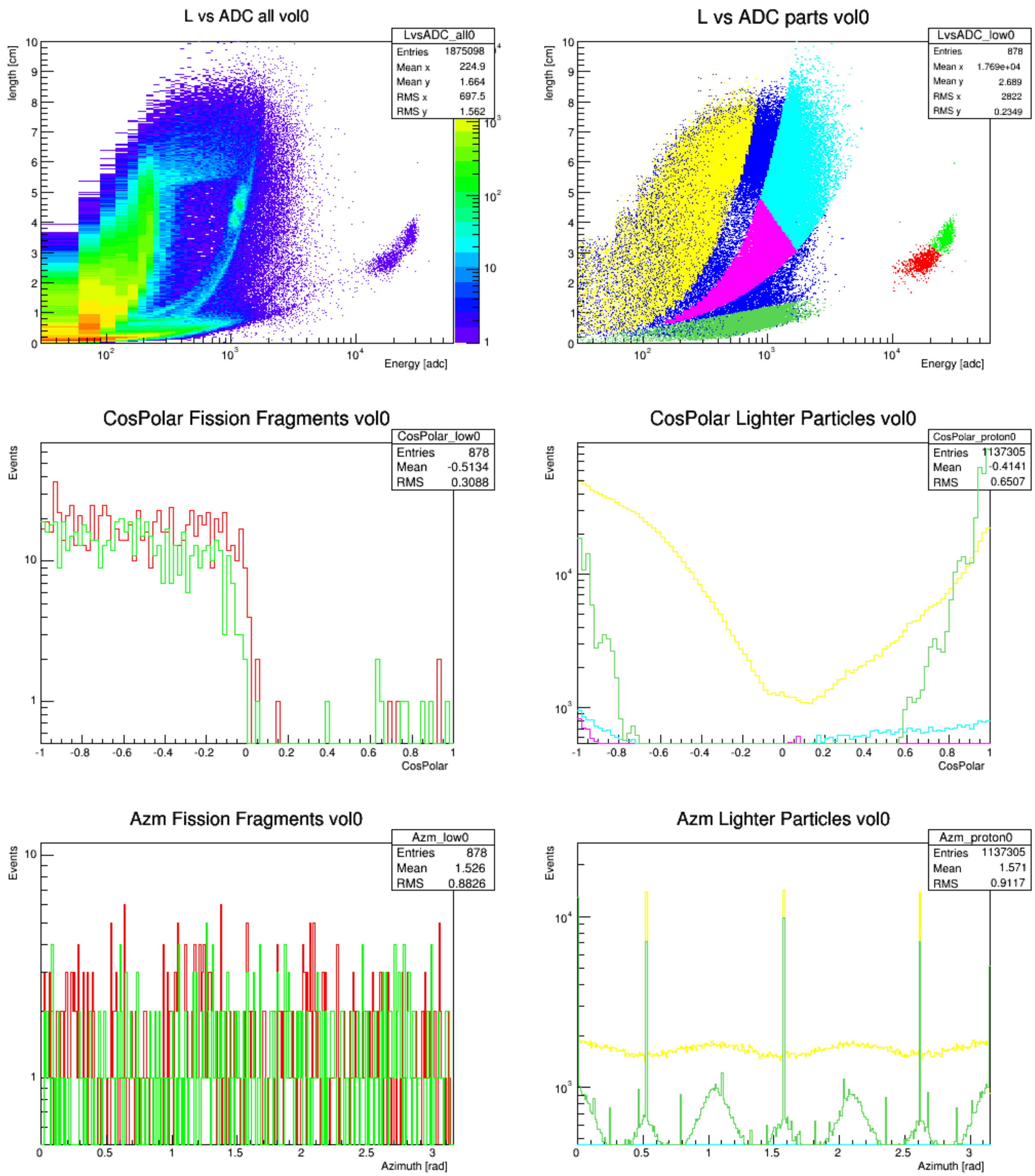

Figure 11: L vs. ADC, CosPolar, and Azm Plots for Fission Fragments (left) and light particles (right) in Volume 0.

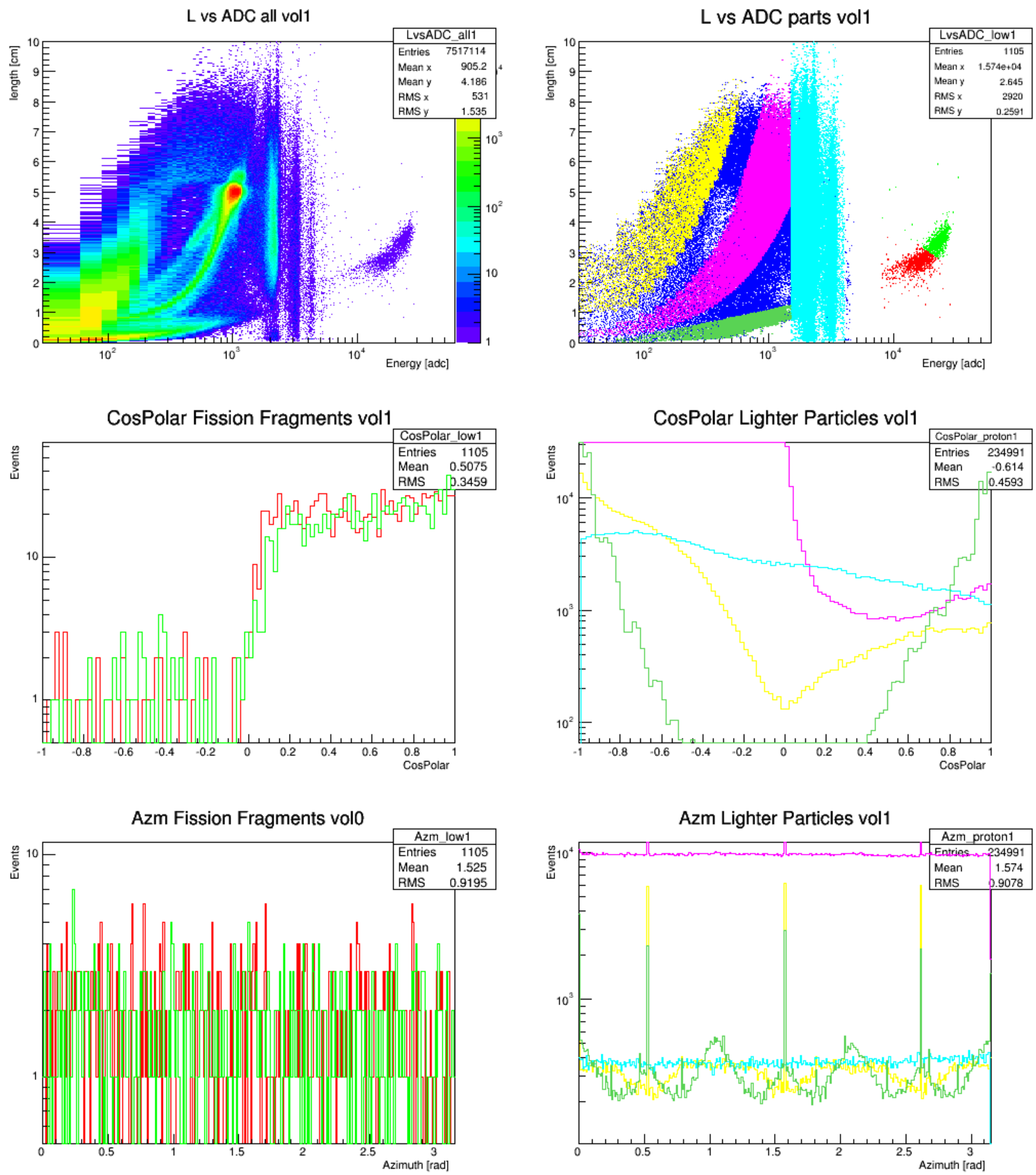

Figure 12: L vs. ADC, CosPolar, and Azm Plots for Fission Fragments (left) and light particles (right) in Volume 1.

The distribution of each fragment is consistent with the theoretical expectation that higher mass fragments will deposit more energy per length of track but won't travel as far because they expend their energy faster. Thus higher mass fragments tend towards the lower right portion of the plots while the lower mass particles tend towards the upper left. The recoil region (green) represents gas atoms that are hit by a neutron, become ionized and move parallel to the beam line. This can be seen in the CosPolar plots, explained below. The stripes (cyan) in volume 1 represent a mix of out-of-time alpha particles that have "piled up" in the detector during a fission event and are only partially recorded. By identifying the characteristics of those tracks we may be able to reduce their contamination in the recorded events.

CosPolar plots are populated on opposite sides of the origin according to the volume.. This reflects the measurement of angles from the forward beam direction, regardless of volume. Angles $\pi/2$ and $3\pi/2$ are the X axis of the FissionTPC. $\mathrm{Cos}(\pi/2) = \mathrm{Cos}(3\pi/2) = 0$ represents the halfway point along the Z axis (Z=0) which divides the FissionTPC chamber into volumes 0 and 1. Neutrons travel along the Z axis to hit the target at Z=0, and many of the particles are emitted along the direction of motion (conservation of momentum). For this run, the thick backing of the target prevents fragments from one side from penetrating into the other volume. So all the activity for a given fission event should be in one volume or the other. This corresponds with Polar Angles between 0 and π, so the horizontal axis of CosPolar ranges from +/-1. This means that for a given volume we should see much more activity on one side of 0 on the horizontal axis than the other. Volume 0 corresponds to negative CosPolar values while Volume 1 corresponds to positive values. Further investigation is needed for the few tracks with CosPolar values on the opposite side of where they are expected. These are probably due to track-fitting errors that can be corrected.

Azimuthal (Azm) plots should have roughly even distribution of counts with respect to the horizontal axis (angle) since there is no preferred direction perpendicular to the beam axis. The spikes in azimuth are likely due to low ADC tracks that need to be removed. Further variation in the azimuthal plots is from dead channels or missing cards. Corrections for these inefficiencies will be applied before the cross-sections are determined.

Figures 13 and 14 show the start and end position of the tracks in volume 0 in the XY plane, while figures 15 and 16 show the same thing for volume 1. Note StartXY and EndXY are distributions at the start and the end of the track for each particle respectively. The upper left two panels in each plot show the uncut and cut regions of the length vs. ADC plots for easy correlation with the remaining panels. In Volume 0, note that fragment start points all lie within the 2 cm target region. Recoil ions in particular track the beam profile very closely, which is elongated and slightly tilted with respect to the horizontal plane. Simulations of the beam profile using the MCNPX program and a precise geometric description of the beam production target and collimators upstream of the FissionTPC match this shape nearly perfectly.[13]

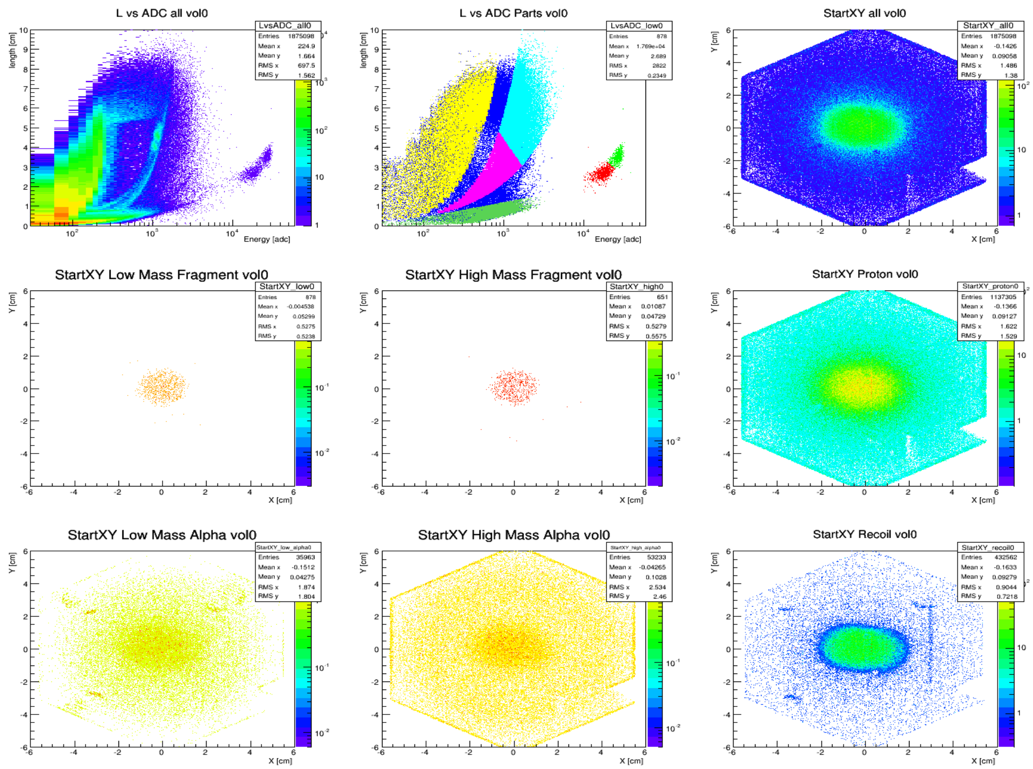

Figure 13: Length vs. ADC and track start positions in the XY plane for all particles and cut regions in Volume 0

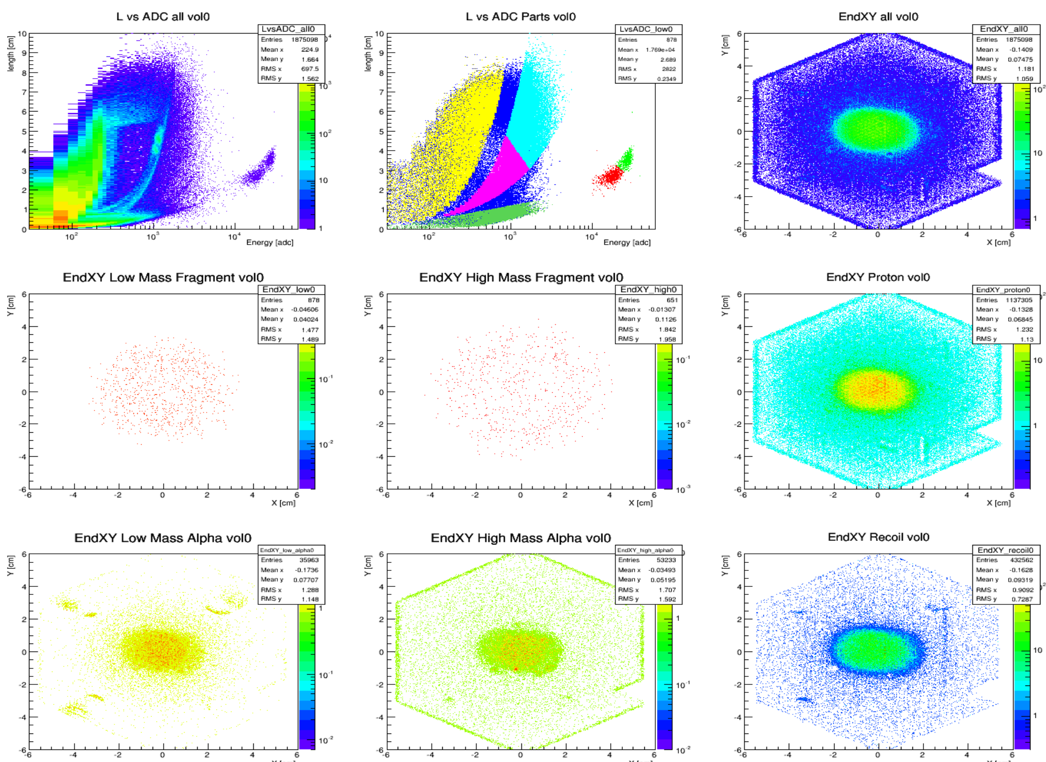

Figure 14: Length vs. ADC and track end positions in the XY plane for all particles and cut regions in Volume 0.

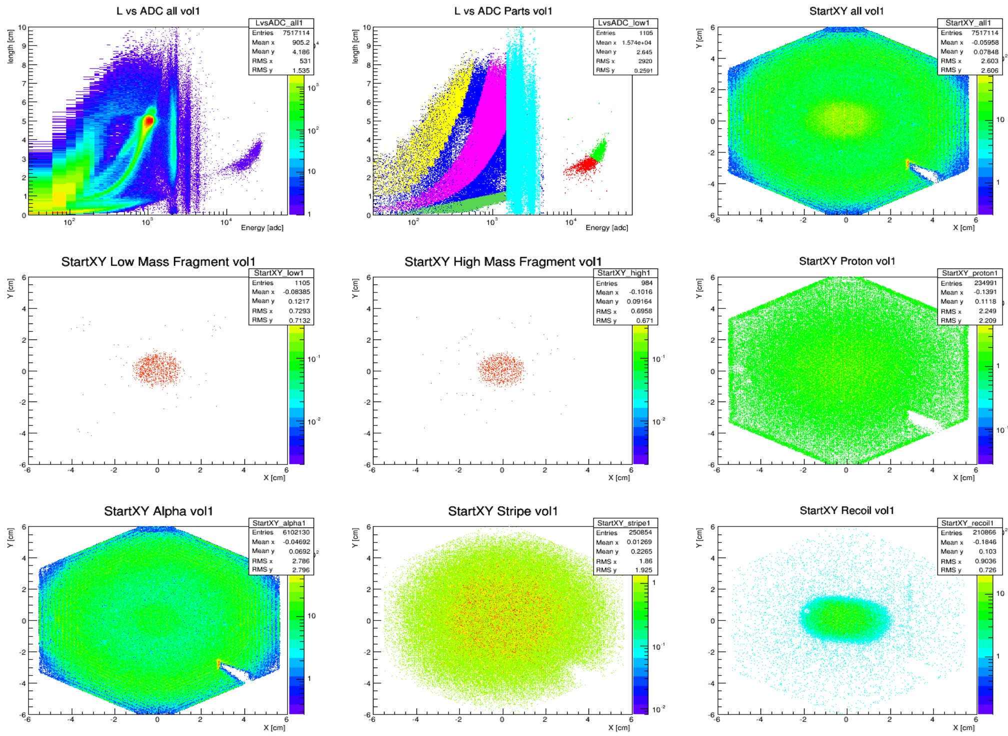

Figure 15: Length vs. ADC and track start positions in the XY plane for all particles and cut regions in Volume 1

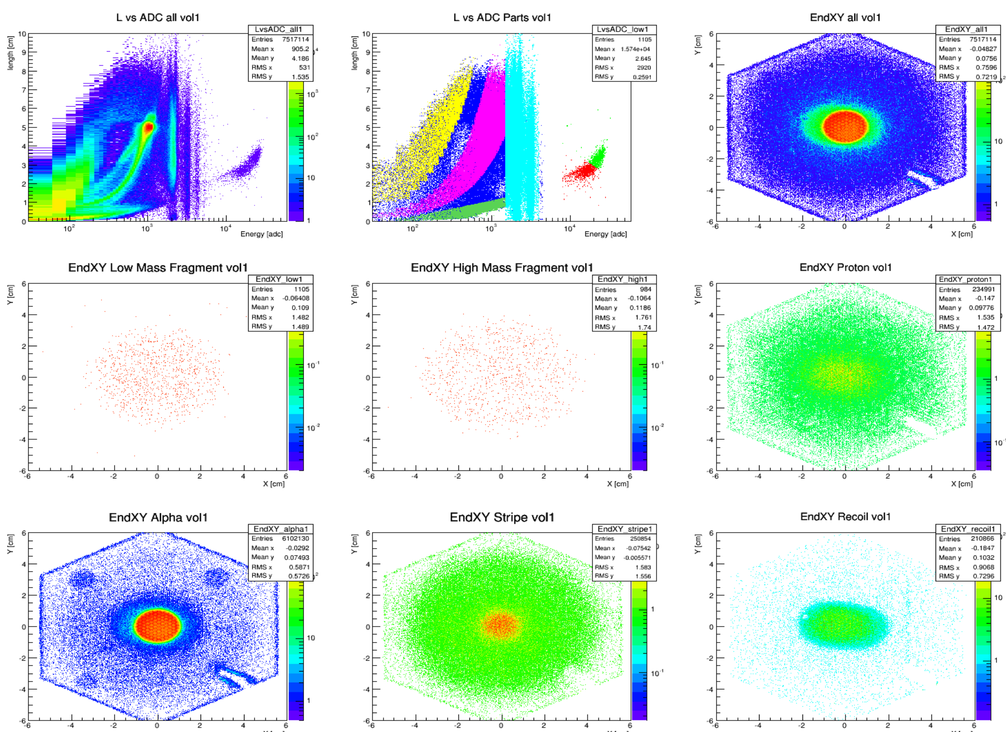

Figure 16: Length vs. ADC and track end positions in the XY plane for all particles and cut regions in Volume 1

The start points for the fragments are tightly coupled to the target in both volumes because the tracking convention is to take the z-position along the track that is closest to the target plane as the start point and the end point is the z-position along the track furthest from the target plane. The plots show this in the spread out locations of the fragment end points. StartXY and EndXY both exhibit an empty spot at the lower right towards the edge of the hexagonal space in both volumes resulting from a faulty or missing EtherDAQ card.

5. Conclusions and Future Work

The data analysis presented here is a first attempt to identify tracking characteristics for different kinds of particles produced in the FissionTPC. By identifying unusual features produced by the tracking software we hope to improve the tracking algorithms so that high-precision fission cross sections can be measured. The CosPolar plots show that we need to improve on direction finding in the FissionTPC. The spikes in the Azm plots show that we need to reduce spurious signals from unphysical tracks. Methods to reduce pile-up alphas and correct missing detector components (cards or channels in this case) must also be developed so that we can detect and measure all events and activity, as shown by the StartXY and EndXY plots. All code used to create plots in this thesis have been checked in to the NIFFTE software version control repository so that future studies may build on this work. Ultimately, the success of the FissionTPC rests on the ability to pinpoint the causes of these anomalies and remove them. The studies presented in this senior thesis represent a first step toward that important goal.

References:

1. Marion Brünglinghaus. "Nuclear fission". European Nuclear Society. Retrieved 2013-01-04
2. "Physics of Uranium and Nuclear Energy." *World Nuclear Association* 01215741 (2014). Tower House. Web. 15 Mar. 2015.
3. "NUCLEAR PHYSICS AND REACTOR THEORY." *DOE FUNDAMENTALS HANDBOOK* 1.1019 (1993). *Energy.gov*. Department of Energy. Web. 15 Mar. 2015.
4. P. Staples, K. Morley, Nuclear Science and Engineering 129 (1998) 149.
5. *A Time Projection Chamber for High Accuracy and Precision Fission Cross Section Measurements*. NIFFTE Collaboration, Nucl. Instrum. Meth. A759 (2014) 50-64.
6. Harris, Randy, and Randy Harris. *Modern Physics*. Second ed. San Francisco: Pearson/Addison Wesley, 2008. Print.
7. Larsen, Delmar. "Nuclear Stability and Magic Numbers." *Nuclear Chemistry*. *The Dynamic Chemistry E-Textbook*. UC Davis. Web. 19 Mar. 2015.
8. Warf, James. *All Things Nuclear*. Second ed. Los Angeles: Figueroa, 2004. Print.
9. Griffiths, David. *Introduction to Elementary Particles*. Second ed. KGaA: WILEY-VCH Verlag GmbH, 2008. Print.
10. Fission Example created by Patric Talou from Los Alamos National Lab (talou@lanl.gov)
11. Paul, Helmut. *Bragg Curve for Alphas in Air*. Digital image. 9 May 2006. Web.
12. "Working Principle of a TPC." *LCTPC* (2015). *A Time Projection Chamber For A Future Linear Collider*. Deutsches Elektronen-Synchrotron DESY. Web. 15 Mar. 2015.
13. MCNPX is a general-purpose Monte Carlo radiation transport code for modeling the interaction of radiation with everything. (https://mcnpx.lanl.gov/)